EPSC Abstracts
Vol. 10, EPSC2015-22, 2015
European Planetary Science Congress 2015

Application of the universal stellar law for the explanation of stability and forms of planet' orbits in exoplanetary systems

A. M. Krot

United Institute of Informatics Problems of National Academy of Sciences of Belarus (alexkrot@vak.org.by; alxkrot @ newman.bas-net.by / Fax: +375-17-3318403)

Abstract

In this work, we consider a statistical theory of gravitating spheroidal bodies to derive and develop the universal stellar law (USL) for extrasolar systems. Previously, the statistical theory for a cosmogonical body forming (so-called spheroidal body) has been proposed in [1-3]. This paper develops USL [4] to explain a stability of the orbital movements of planets as well as the forms of planetary orbits with regard to the Alfvén's oscillating force in the Solar system and other exoplanetary systems.

In 1911–24 the astronomers Russell, Hertzsprung and Eddington established that there is a dependence of luminosity of a star on temperature of its stellar surface for stars of the Main sequence (the diagram of Hertzsprung–Russell), and also there is a connection between luminosity and mass of star (the diagram of mass–luminosity) [5]. Recently Pintr et al. [6] have found heuristic regression dependences and applied the regression analysis to estimation of physical parameters of stars. Thereupon there is a question*: whether there exist like the Kepler's laws the universal law for the planetary systems connecting temperature, size and mass of each of stars?*

According to the statistical theory of gravitating spheroidal bodies [1-3] under the usage of laws of celestial mechanics (especially, for stars) it is necessary to take into account the stellar corona. Moreover, the parameter of gravitational compression α of a spheroidal body [1-3] (describing the Sun, in particular) has been estimated by the linear size of its core, i.e. by the thickness of a visible part of the solar corona [4].

Using the conception of gravitating spheroidal body, this work derives the equation of state of an ideal stellar substance:

$$\sqrt{\alpha}\cdot M = \frac{\kappa \bar{i}}{m_{\mathrm{p}}\bar{\mu}_{\mathrm{r}}}\cdot T\,, \qquad (1)$$

where α is a parameter of gravitational compression, M and T are stellar mass and temperature respectively, $\bar{i}$ is a mean number of freedom degree of a moving particle in the highly ionized stellar substance, $\bar{\mu}_{\mathrm{r}}$ is its mean relative molecular weight, m_{p} is the mass of proton, and κ is the introduced *universal stellar constant* [4]:

$$\kappa = 3\sqrt{\pi}\cdot\frac{k_{\mathrm{B}}}{\gamma} \approx 1.10003963\cdot 10^{-12}\,(\mathrm{kg}^2/\mathrm{K}\cdot\mathrm{m})\,,$$

where k_{B} and γ are the constants of Boltzmann and Newton respectively. The equation (1) has been named so by analogy to the known Clapeyron–Mendeleev' equation of state of an ideal gas. The stars obeying the equation of state of an ideal stellar substance (1) we can call as *ideal* ones.

Using this equation, we obtain USL for the planetary systems connecting temperature, size and mass of each of stars:

$$\sqrt{\alpha}\cdot\frac{\overline{\mu}_{\mathrm{r}}}{\overline{i}}\cdot\frac{m_{\mathrm{p}}M}{T}=\mathrm{const}. \qquad (2)$$

Obviously, a verification of USL (2) for different stars requires estimating their parameters $\sqrt{\alpha}$, M , T and also $\overline{\mu}_{\mathrm{r}}$, i.e. chemical composition of stars [4]. Since USL is based on the Poincaré's virial theorem applicable to a cloud-like configuration of ideal gas as the gravitating spheroidal body in a mechanic equilibrium state then the question *how long the gravitational field of star remains stable* is actual. Naturally, the stabilities as well as forms of planetary orbits depend on a constancy of the gravitational field level around a star directly. As Alfvén and Arrhenius noted, "the circular motion with period T is usually modified by superimposed oscillations. Radial oscillations (in the preferred plane) with period $\approx T$ change the circle into an ellipse with eccentricit e .Axial oscillations (perpendicular to the preferred plane), also with a period $\approx T$, make the orbit inclined at an angle i to this plane" [7].

This work explains an origin of the Alfvén's oscillating forces modifying forms of planetary orbits within the framework of the statistical theory of gravitating spheroidal bodies. Concretely, this paper shows that temporal deviation of the gravitational compression function of a spheroidal body (modeling a gas-dust protoplanetary cloud) induces the additional periodic forces making the orbits elliptic ones. Moreover, the temporal deviation of the gravitational compression function leads to the special cases periodically when the additional periodic force becomes counterbalance to the gravitational force, i.e. the principle of anchoring mechanism occurs. Owing to this principle, the stability of planetary orbits is realized in extrasolar systems.

This work also notes that knowledge of some characteristics for multi-planet extrasolar systems permits us to refine own parameters of stars. Really, the numerous papers are devoted to investigations of exoplanetary systems in the last time (for example, [6, 8-10]). In this connection, comparison with estimations of temperatures using USL for multi-planet extrasolar systems testifies the obtained results entirely.

References

[1] Krot, A.M.: 2009, A statistical approach to investigate the formation of the solar system. *Chaos, Solitons and Fractals* **41** (3), 1481-1500.

[2] Krot, A. M.: 2012, *A Statistical Theory of Formation of Gravitating Cosmogonic Bodies*. Minsk, Bel. Navuka, 448p. – ISBN 978-985-08-1442-5 [monograph in Russian].

[3] Krot, A.M.: 2012, A model of forming planets and distribution of planetary distances and orbits in the solar system based on the statistical theory of spheroidal bodies. In: *Solar System: Structure, Formation and Exploration*, ch.9 (Ed. by Matteo de Rossi). New York, Nova Science Publishers, pp. 201-264. – ISBN: 978-1-62100-057-0.

[4] Krot, A. M.: 2014, On the universal stellar law for extrasolar systems. *Planetary and Space Science* **101C**, 12-26.

[5] Jeans, J.: 1929, *Astronomy and Cosmogony*. Cambridge, University Press.

[6] Pintr, P., Peřinová, V., Lukš, A., Pathak, A.: 2013, Statistical and regression analyses of detected extrasolar systems. *Planetary and Space Science* **75** (1), 37-45.

[7] Alfvén, H., Arrhenius, G.: 1970, Structure and evolutionary history of the solar system. I. *Astrophys. Space Sci.* **8**, 338-421.

[8] Lovis, C., Mayor, M., Pepe, F., et al.: 2006, An extrasolar planetary system with three Neptune-mass planets. *Nature* **441** (7091), 305-309.

[9] Wittenmyer, R.A., Endl, M., Cochran, W.D.: 2007, Long-period objects in the extrasolar planetary systems 47 Ursae Majoris and 14 Herculis. *Astrophysical Journal* **654**, 625-632.

[10] Lovis, C., Segransan, D., Mayor, M., et al.: 2011, The HARPS search for southern extra-solar planets – XXVII. Up to seven planets orbiting HD 10180: probing the architecture of low-mass planetary systems. *Astronomy & Astrophysics* **528**, A112.

EPSC Abstracts
Vol. 10, EPSC2015-116, 2015
European Planetary Science Congress 2015

Magnetic moment and plasma environment of exoplanets as determined from Lyα observations

K.G. Kislyakova (1), H. Lammer (1), M. Holmström (2), P. Odert (1) and M.L. Khodachenko (1)
(1) Space Research Institute, Austrian Academy of Sciences, Graz, Austria,
(2) Swedish Institute of Space Physics, Kiruna, Sweden
(kristina.kislyakova@oeaw.ac.at)

Abstract

We present an indirect method for estimate of exoplanetary magnetic moment based on Lyα observations in combination with the consequent numerical modelling and analysis [1, 2].

1. Introduction

Transit observations of HD 209458b in the stellar Lyman-α (Lyα) line revealed strong absorption in both blue and red wings of the line interpreted as hydrogen atoms escaping from the planet's exosphere at high velocities. The following sources for the absorption were suggested: acceleration by the stellar radiation pressure, natural spectral line broadening, charge exchange with stellar wind. We reproduce the observation by means of modelling that includes all aforementioned processes. Our results support a stellar wind with a velocity of $\approx$ 400 km$\times$s^{-1} at the time of the observation and a planetary magnetic moment of $\approx 1.6 \times 10^{26}$ A$\times$m^2.

2. Method

The particle code is based on Direct Simulation Monte Carlo (DSMC) method and includes stellar wind protons and atmospheric neutrals presented by metaparticles. We include also radiation pressure, gravitational effects (gravity, Coriolis, centrifugal, tidal forces), charge-exchange between protons and neutrals and elastic collisions between neutrals. The code allows to study the interaction processes in the exosphere under different conditions for magnetized and non-magnetized bodies. As a result the distribution of neutrals and ions around the planet and the location of the magnetospheric obstacle is obtained. Afterwards we apply post-processing programs developed to estimate the Lyα attenuation produced by neutral cloud around an exoplanet and observed in-transit.

3. Results

As an example of the simulation result we shown a slice of a 3D hydrogen cloud around HD 209458b (Fig. 1). The star is on the right. The red and blue dots correspond to H^+ ions and neutral hydrogen atoms, respectively. The black dot represents the planet. The white empty area around the planet is the lower atmosphere which is not considered in this study.

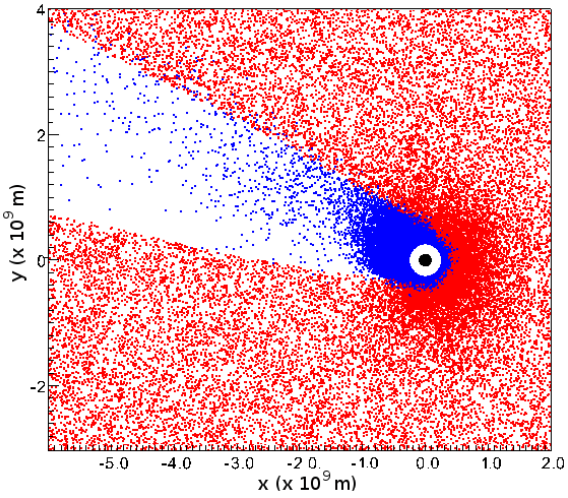

Figure 1: An example of modelled neutral hydrogen cloud around HD 209458b [1].

After a hydrogen corona is modelled, we apply the post-processing software to calculate the Lyα absorption caused by the cloud during the planetary transit, which is then compared to the observations [1, 2, 3]. When the observations are reproduced with a good precision (Fig. 2), we assume the obtained magnetic obstacle to estimate the planetary magnetic moment in a dipole approximation using the formula [4]

$$\mathcal{M} = \left(\frac{8\pi^2 R_{\rm s}^6 \rho_{\rm sw} v_{\rm rel}^2}{\mu_0 f_0^2} \right)^{1/2} . \quad (1)$$

Here, $R_{\rm s}$ is the magnetospheric stand-off distance, μ_0 is the diamagnetic permeability of free space, $f_0 \approx 1.22$ is a form factor of the magnetosphere, $\rho_{\rm sw}$ is the mass density of the stellar wind, and $v_{\rm rel}$ is the relative velocity of the stellar wind plasma, including the planetary orbital velocity. The parameters $R_{\rm s}$, $\rho_{\rm sw}$, and $v_{\rm rel}$ are obtained from the modelling.

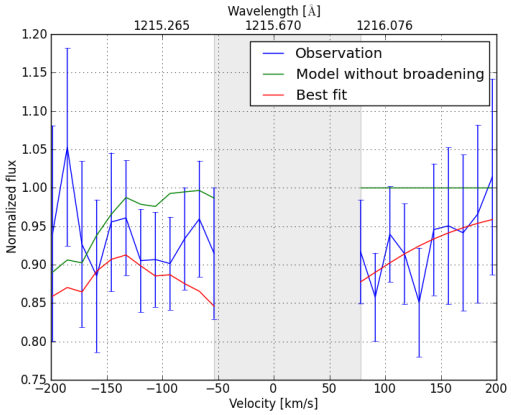

Figure 2: Comparison of modelled and observed (according to Ben-Jaffel and Hosseini[3]) Lyα spectra at mid-transit [1]. The blue lines show the observation, the red and green lines - best-fit modelling with and without Doppler line broadening, respectively. The region in the center contaminated by the geocoronal emission is excluded.

In the case of a close-in obstacle, the exosphere interacts directly with the stellar wind. This diminishes the number of H neutrals, first by charge exchange and second by stellar wind electron impact ionization. A stronger intrinsic field shifts the magnetic boundary away from the planet and effectively protects the atmosphere from these processes. This increases the number of neutrals undergoing acceleration by radiation pressure and leads to overabsorption in comparison to the in-transit observation. The stellar wind speed influences the speed of the newly produces energetic neutral atoms and can be defined from the spectral signatures in the Lyα line as well.

4. Summary and Conclusions

We presented an indirect method, which can be used to estimate the total magnetic moment of exoplanets, as well as restrict the stellar wind parameters at the time of observation. The methodology is of a particular interest considering the lack of the direct measurements of exoplanetary magnetic moments at present. The method was successively applied to the Hot Jupiter HD 209458b [1] and predicted the magnetic moment of the planet of $\approx$ 10% of the one of Jupiter. Also, the model predicted a fast stellar wind at the time of observation ($\approx$ 400 km/s).

The method can be applied to every exoplanet for which the Lyα observations are available.

Acknowledgements

This study was carried out with the support by the FWF NFN project S116 001-N16 "Pathways to Habitability: From Disk to Active Stars, Planets and Life" and the related FWF NFN subprojects, S116 04-N16 , S116 06-N16, and S116 07-N16.

References

[1] Kislyakova, K.G., Holmström, M., Lammer, H, Odert, P., and Khodachenko, M.L.: Magnetic moment and plasma environment of HD 209458b as determined from Lyα observations, Science, vol. 346, p. 981, 2014.

[2] Holmström, M., Ekenbäck, A., Selsis, F., Penz, T., Lammer, H., Wurz, P.: Energetic neutral atoms as the explanation for the high-velocity hydrogen around HD 209458b, Nature, Vol. 451, p. 970, 2008.

[3] Ben-Jaffel, L., Hosseini, S.S.: On the existence of energetic atoms in the upper atmosphere of exoplanet HD209458b, Astrophys. J. vol. 709, p. 1284, 2010.

[4] Khodachenko, M.L., Alexeev, I., Belenkaya, E., Lammer, H., Griessmeier, J.-M., Leitzinger, M., Odert, P., Zaqarashvili, T., and Rucker, H.O.: Magnetospheres of "Hot Jupiters": the importance of magnetodiscs in shaping a magnetospheric obstacle, Astrophys. J. vol. 744, p. 70, 2012.

EPSC Abstracts
Vol. 10, EPSC2015-242, 2015
European Planetary Science Congress 2015

On the Io-type plasma source in Hot Jupiters systems

K.G. Kislyakova (1), E. Pilat-Lohinger (2), B. Funk (2), H. Lammer (1), N.V. Erkaev (3,4), and M. Boudjada (1)
(1) Space Research Institute, Austrian Academy of Sciences, Graz, Austria
(2) University of Vienna, Department of Astrophysics, Vienna, Austria
(3) Institute of Computational Modelling, Krasnoyarsk, Russian Federation
(4) Siberian Federal University, Krasnoyarsk, Russian Federation
(kristina.kislyakova@oeaw.ac.at)

Abstract

We discuss the possibility of the existence of Io-type plasma source in the exoplanetary systems from the stability point of view. We point out that close-in exoplanets possibly have no or only very small moons because of the small Hill radii defined by their proximity to the host stars. For close-in Hot Jupiters, the Hill radius is of the order of only several planetary radii. Some exoplanets, e.g. WASP-12b, are so inflated, that they are believed to fill their Roche lobes with the expanded atmosphere only. For stability reasons, the orbits of the moons have to be within the Hill sphere of their planets, this makes the very existence of the Earth- and even Io-size moons in such systems questionable, and, thus, probably also the Io-type plasma source. However, one can not exclude plasma producing exomoons orbiting in or near the Lagrange points L4 and L5. We discuss also the outgassing rates of such an exomoon in comparison to Io.

1. Introduction

WASP-12b is a planet which showed a significant early ingress in UV observations [1]. This result was later confirmed [2]. The following sources for the absorption were suggested: the optically dense material in the vicinity of a planetary bow shock [1, 2] and a plasma torus outgassed by an exomoon of the size of Io, assuming the same outgassing rate [3]. The same plasma torus hypothesis was also applied to HD 189733b.

In this work, we compare the Jupiter satellite system to those suggested at Hot Jupiters WASP-12b and HD 189733b. We study potential orbits of these satellites from the dynamical point of view and discuss possible outgassing rates a satellite may have in a Hot Jupiter system compared to Io.

2. Method

We study the stability of the satellites by means of numerical simulations using a Bulirsch-Stoer integration method with adaptive stepsize. In addition to the orbit, we calculate the variation equations for the tangent vectors whose evolution defines the orbital behavior via the FLI (Fast Lyapunov Indicator), a chaos indicator which was introduced in an earlier study [4]. Taking into account the architecture of the considered Hot Jupiter systems and assuming different orbital parameters and mass of the satellites, we analyse the extension of the stability zones around L4 and L5 in the circular restricted and in the three body problem. Our results are in agreement with an earlier study [5].

3. Results

Fig. 1 shows the dependence of the maximal possible separation between an exoplanet and its satellite on the planet's orbital distance assuming three different mass ratios between the planet and the star.

4. Summary and Conclusions

Considering small possible masses of the exomoons in Hot Jupiters systems, one has to reinvestigate the possible outgassing rate a small moon can produce in comparison to Io. Also, one has to take into account the small orbital separation between an exomoon and a Hot Jupiter needed for the stability of the exomoon orbit and/or its possible short life time. These factors together make the explanation of the early egress observed at WASP-12b by plasma outgassing from an exomoon rather unrealistic.

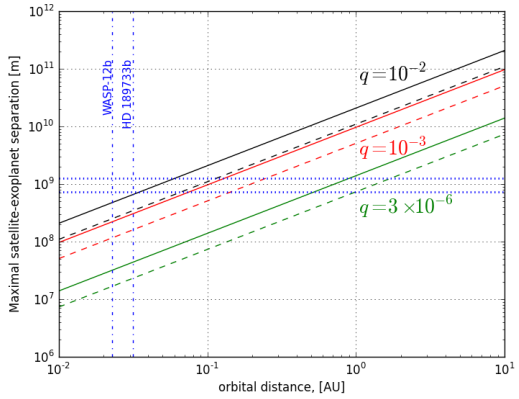

Figure 1: Maximal possible separation for retrograde (solid lines) and prograde (dashed lines) satellites depending on the orbital separation for three possible values of planet-star mass ratio $q = 10^{-2}; 10^{-3}; 3 \times 10^{-6}$ (black, red, green lines, respectively).

Acknowledgements

This study was carried out with the support by the FWF NFN project "Pathways to Habitability: From Disk to Active Stars, Planets and Life" and the related FWF NFN subprojects S116 08-N16 and S116 07-N16.

References

[1] Fossati, L., Haswell, C.A., Froning, C.S., et al.: Metals in the exosphere of the highly irradiated planet WASP-12b, Astrophys. J., vol. 714, L222, 2010.

[2] Haswell, C.A., Fossati, L., Ayres, T., et al.: Near-ultraviolet absorption, chromospheric activity, and star-planet interactions in the WASP-12 system, Astrophys. J., vol. 760, p. 79, 2012.

[3] Ben-Jaffel, L., and Ballester, G. E.: Transit of exomoon plasma tori: new diagnosis, Astrophys. J., vol. 785, L30, 2014.

[4] Froeschle, Cl., Gonszi, R., and Lega, E.: The fast Lyapunov indicator: a simple tool to detect weak chaos. Application to the structure of the main asteroidal belt, PSS, vol. 45, p. 881, 1997.

[5] Domingos, R. C., Winter, O. C., and Yokoyama, T.: Stable satellites around extrasolar giant planets, MNRAS, vol. 373, p. 1227, 2006.

EPSC Abstracts
Vol. 10, EPSC2015-293, 2015
European Planetary Science Congress 2015

Orbital evolution of viscoelastic bodies: effect of internal structure

M. Káňová, M. Běhounková
Charles University in Prague, Faculty of Mathematics and Physics, Department of Geophysics, Czech Republic
(kanova@karel.troja.mff.cuni.cz)

Abstract

Tidal evolution of planetary orbit and rotation has been traditionally described using specific rheological assumptions: constant phase lag [1] or constant time lag [2]. Such rheologies are, however, unsuitable in the case of terrestrial bodies described by realistic viscosity and rigidity (e.g. [3]), as they predict stable pseudo-synchronous, non-resonant rotation of planets on eccentric orbit, which is not observed in the nature (planetary satellites in the Solar system, planet Mercury). Several authors have recently proposed analytical treatment of orbital evolution with the assumption of a viscoelastic rheology ([3], [4]). Here, we present a numerical approach to the problem and we study the effects of viscosity pattern on the rate of tidal dissipation.

1. Introduction and methods

Unperturbed system of two spherically symmetric bodies maintains constant orbital parameters, determined uniquely by the solution of a two-body problem. The orbital evolution can emerge only when a perturbation is introduced into the system. Such perturbation arises, in our case, as a result of tidal deformation of the planet, breaking off its spherical symmetry.

We therefore first investigate the deformation of a planetary mantle undergoing tidal loading by a host star. The mantle is represented by a viscoelastic Maxwell-like spherical shell and its response to the loading force $\mathbf{f}$ is computed in the time domain as a solution of governing equations

$$\nabla \cdot \mathbf{u} = 0\,, \tag{1}$$

$$-\nabla\pi + \nabla\cdot\mathbf{D} + \mathbf{f} = \mathbf{0}\,, \tag{2}$$

$$\frac{\partial \mathbf{D}}{\partial t} - \frac{\partial}{\partial t}\left[\mu(\nabla\mathbf{u} + \nabla^{\mathrm{T}}\mathbf{u})\right] = -\frac{\mu}{\eta}\mathbf{D}\,, \tag{3}$$

where $\mathbf{u}$ is the displacement vector, π and $\mathbf{D}$ represent the isotropic and the deviatoric part of the stress tensor, μ is the effective shear modulus and η the effective viscosity [5]. The force $\mathbf{f}$ consist of two contributions: the first one due to the external potential and the second one due to the self-gravity of a deformed planet. We solve the equations using a spherical harmonic decomposition in the lateral direction and a staggered finite difference method in the radial direction [6].

The mass excess or deficit due to the boundary deflections of a deformed shell enables us to compute the disturbation of the external field. The disturbing force $\mathbf{f}_{\mathrm{dist}}$ is evaluated in the instantaneous position of a host star and decomposed into three orthogonal components: $\mathbf{R}$ in the direction of radius vector, $\mathbf{S}$ perpendicular to $\mathbf{R}$ in the orbital plane, pointing in the direction of planetary motion, and $\mathbf{W}$ perpendicular to the orbital plane, pointing in the direction of orbital angular momentum. Perturbation of the planetary orbit for a system containing one star and one planet is then computed using Gauss planetary equations:

$$\frac{\mathrm{da}}{\mathrm{dt}} = \frac{2}{n\sqrt{1-e^2}}\left[eR\sin\nu + \frac{p}{r}S\right]\,, \tag{4}$$

$$\frac{\mathrm{de}}{\mathrm{dt}} = \frac{\sqrt{1-e^2}}{nae}\left[eR\sin\nu + \left(\frac{p}{r} - \frac{r}{a}\right)S\right]\,. \tag{5}$$

Here a and e symbolize the semi-major axis and the eccentricity, respectively, n is the mean motion of the planet, ν the true anomaly, r represents the instantaneous distance of the planet from the star, $p = a(1-e^2)$ is the semi-latus rectum and R, S are the magnitudes of the first two components of the disturbing (tidal) force.

Once we know the average values of secular change in a and e, we compute the long-term orbital evolution explicitly. The rotational period Ω of a spherical planet with the moment of inertia C evolves in agreement with the conservation of total angular momentum

of the system.

$$\frac{Mm}{M+m}\, a^2 n \sqrt{1-e^2} \;+\; C\Omega \;=\; \text{const.} \qquad (6)$$

2. Spin-orbit resonances

Study of the long-term evolution of any planetary processes depending on the surface temperature and/or tidal loading requires realistic model for the orbital evolution. Locking of a planet into a spin-orbit resonance results in insolation and temperature pattern that is qualitatively different from that of pseudo-synchronous state.

Figure 1 shows stable spin-orbit ratios for a close-in terrestrial planet with various values of eccentricity and effective viscosity (note that the effective viscosity for tidal deformation is lower than the viscosity used in mantle convection models—the mean effective viscosity of the Earth mantle would be $\sim 10^{18}$ Pa.s). The results demonstrate that while for some values of viscosity η and Maxwell time $\tau_M = \frac{\eta}{\mu}$ the equillibrium rotation state is well described by the constant time lag model (purely viscous or elastic limit), other Maxwell bodies tend to get locked into spin-orbit resonance. The upper left plot of Figure 1 depicts an intermediate state between discrete spin-orbit resonances and pseudo-synchronous rotation, a result for a viscoelastic planet with very low viscosity.

3. Summary and Conclusions

We have implemented a numerical model for the orbital and rotational evolution of viscoelastic planets and studied parameter dependence of tidal dissipation and stable spin-orbit ratios, including resonances. The model enables evaluation of effects of the internal viscosity structure of the planet and may be useful in further studies of coupled internal and orbital evolution.

Acknowledgements

This work was supported by the Grant Agency of Charles University (project No. 338214) and the Czech Science Foundation (project No. 14-04145S).

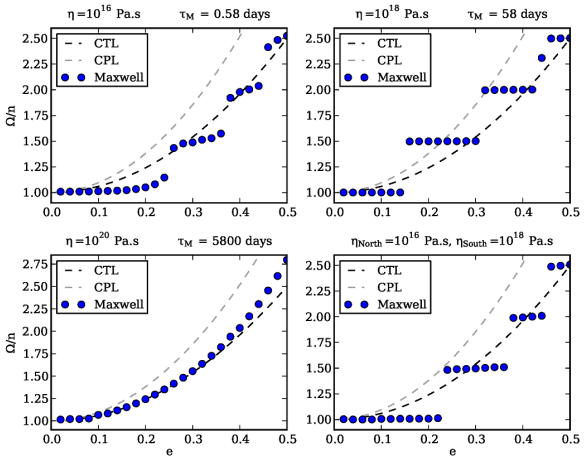

Figure 1: Stable spin-orbit ratios as a function of eccentricity for different values of effective viscosity. Comparison with traditional models: CTL = constant time lag, CPL = constant phase lag. Earth-like planet orbiting Sun-like star, $a = 0.055\,\text{AU}$, $T_{orb} = 4.71\,\text{days}$, $\mu = 2.10^{11}$ Pa.

References

[1] Kaula, W. M.: *Tidal Dissipation by Solid Friction and the Resulting Orbital Evolution*, Reviews of Geophysics 2, pp. 661-685, 1964.

[2] Mignard, F.: *The evolution of the lunar orbit revisited*, The Moon and the Planets 20, pp. 301-315, 1979.

[3] Makarov, V. V., Efroimsky, M.: *No pseudosynchronous rotation for terrestrial planets and moons*, The Astrophysical Journal 764:27, 2013.

[4] Correia, A. C. M., Boué, G., Laskar, J., Rodríguez, A.: *Deformation and tidal evolution of close-in planets and satellites using a Maxwell viscoelastic rheology*, Astronomy & Astrophysics 571, A50, 2014.

[5] Běhounková, M., Tobie, G., Choblet, G., Čadek, O.: *Coupling mantle convection and tidal dissipation: Applications to Enceladus and Earth-like planets*, Journal of Geophysical Research 115, E09011, 2010.

[6] Tobie, G., Čadek, O., Sotin, C.: *Solid tidal friction above a liquid water reservoir as the origin of the south pole hotspot on Enceladus*, Icarus 196, pp. 642–652, 2008.

EPSC Abstracts
Vol. 10, EPSC2015-295, 2015
European Planetary Science Congress 2015

Surface temperature and tidal heating on close-in exoplanets

M. Káňová, M. Běhounková
Charles University in Prague, Faculty of Mathematics and Physics, Department of Geophysics, Czech Republic
(kanova@karel.troja.mff.cuni.cz)

Abstract

Close-in terrestrial exoplanets are subjected to strong stellar tides resulting in tidal dissipation and locking into spin-orbit resonances. The presence of significant tidal heating can lead to extensive temperature increase and possibly to thermal runaways within the planetary interior. Additionally, the planets locked in the spin-orbit resonance may exhibit large surface temperature contrasts which further influence the temperature pattern and heat transport. Here, we focus on the parameter dependence of both quantities—the surface temperature and the tidal heating—and discuss the significance of the spin-orbit resonances.

1. Model and Methods

In order to compute the surface temperature of a planet, we solve the heat diffusion equation along the orbit using a finite difference method with staggered grid for the spatial discretization and Crank-Nicolson scheme for the time discretization. The temperature field $T(r, \vartheta, \varphi)$ is computed in a thin subsurface layer (up to few meters) under the assumption that the planet possesses no atmosphere and its surface is covered by regolith. The upper boundary condition for the heat equation is given by the energy conservation law

$$S(1-A) = \varepsilon\sigma T^4 - k\frac{\partial T}{\partial r}\,, \qquad (1)$$

where k is the thermal conductivity, A and ε are the albedo and the emissivity, respectively, and σ is the Stefan-Boltzman constant. The instantaneous insolation $S(\vartheta, \varphi)$ is a function of orbital and rotational parameters (semi-major axis, eccentricity of the orbit, obliquity, spin rate) [1].

Computation of the tidal heating requires knowledge of the rate of energy dissipation in the planetary mantle. Average power over a time interval T due to the heating may be obtained from the deviatoric part $\mathbf{D}$ of the Cauchy stress tensor and the strain rate tensor $\dot{\epsilon}$ as

$$P = \frac{1}{T}\int_V \int_t^{t+T} \dot{\epsilon}(\tau) : \mathbf{D}(\tau)\mathrm{d}\tau\mathrm{d}V\,. \qquad (2)$$

The tidal deformation of the planet is evaluated for the Maxwell or the Andrade viscoelastic rheology [2], using a staggered finite difference method in the radial direction and spherical harmonic decomposition in the lateral directions.

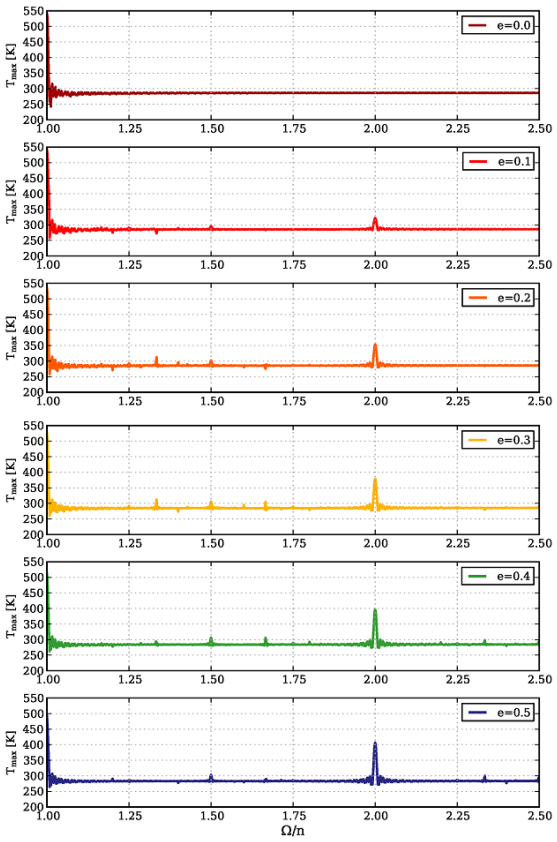

Figure 1: Mean temperature in a point of planetary surface with the maximum average insolation. Effect of the spin-orbit ratio (x-axis) and the eccentricity (colour).

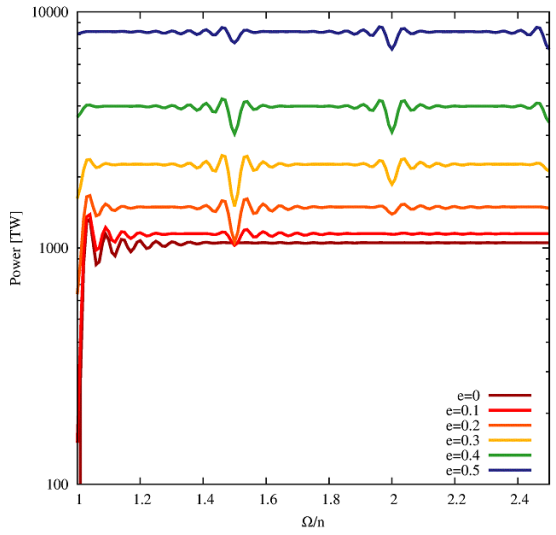

Figure 2: Average tidal heating as a function of the spin-orbit ratio and the eccentricity.

2. Results

Figure 1 and Figure 2 show results obtained for an Earth-like planet orbiting a host star with the mass $M_* = 0.5\,\mathrm{M_{Sun}}$ on the orbit with the semi-major axis $a = 0.1\,\mathrm{AU}$. The emissivity of the planetary surface is $\varepsilon = 0.9$, the albedo is $A = 0.1$ and the planet is considered to be a Maxwell body with the effective viscosity [2] $\eta = 10^{18}\,\mathrm{Pa.s}$ and the effective shear modulus $\mu = 2.10^{11}\,\mathrm{Pa}$.

The most prominent features in our parametric study of the surface temperature and the tidal heating are associated with the spin-orbit resonances. When the planet gets tidally locked and its rotational frequency is an integer multiple of the orbital frequency, the average temperature at the most irradiated location on the planetary surface increases abruptly in the order of hundreds of kelvins (Figure 1). Weaker effect is observed for other half-integer or third-integer multiples. The tidal heating of the planetary mantle (Figure 2), on the other hand, reaches a local minimum when the spin rate equals half-integer multiple of the orbital frequency, the deepest minimum being associated with the stable spin-orbit resonance for a given eccentricity, semi-major axis and the Maxwell time. Planets with lower eccentricity of the orbit are expected to be locked in a synchronous rotation state (1:1 spin-orbit resonance), while planets on the eccentric orbits prefer higher spin-orbit resonances [3].

3. Summary and Conclusions

We have studied the parameter dependence of the surface temperature and the tidal heating on terrestrial exoplanets without atmosphere. Both quantities undergo significant change when the planet falls into a spin-orbit resonance. This may have important consequences for the type of mantle convection as well as for possible habitability of the planet (if the atmosphere was considered), as it would be altered during the orbital evolution.

Acknowledgements

This work was supported by the Grant Agency of Charles University (project No. 338214) and the Czech Science Foundation (project No. 14-04145S).

References

[1] Dobrovolskis, A.R.: *Insolation on exoplanets with eccentricity and obliquity*, Icarus 204, pp. 760-776, 2013.

[2] Běhounková, M., Tobie, G., Choblet, G., Čadek, O.: *Coupling mantle convection and tidal dissipation: Applications to Enceladus and Earth-like planets*, Journal of Geophysical Research 115, E09011, 2010.

[3] Káňová, M. and Běhounková, M.: *Orbital evolution of viscoelastic bodies: effect of internal structure*, EPSC, 2015.

EPSC Abstracts
Vol. 10, EPSC2015-307, 2015
European Planetary Science Congress 2015

Modelling the ionosphere of gas-giant exoplanets irradiated by low-mass stars

J. Chadney (1), M. Galand (1), Y. Unruh (1), T. Koskinen (2) and J. Sanz-Forcada (3)
(1) Department of Physics, Imperial College London, UK, (2) Lunar and Planetary Laboratory, University of Arizona, USA, (3) Centro de Astrobiologia (CSIC-INTA), Madrid, Spain
(joshua.chadney10@imperial.ac.uk)

Abstract

The composition and structure of the upper atmosphere of Extrasolar Giant Planets (EGPs) are affected by the high-energy spectrum of the host star from soft X-rays to Extreme UltraViolet (EUV) (0.1-10 nm). This emission depends on the activity level of the star, which is primarily determined by its age [1]. In this study, we focus upon EGPs orbiting K- and M-dwarf stars of different ages. XUV spectra for these stars are constructed using a coronal model [2]. These spectra are used to drive both a thermospheric [3] and an ionospheric model, providing densities of neutral and ion species. Ionisation is included through photo-ionisation and electron-impact processes. The former is calculated by solving the Lambert-Beer law, while the latter is calculated from a supra-thermal electron transport model [4]. Planets orbiting far from the star are found to undergo Jeans escape, whereas close-orbiting planets undergo hydrodynamic escape. The critical orbital distance of transition between the two regimes is dependent on the level of stellar activity. We also find that EGP ionospheres at all orbital distances considered (0.1-1 AU) and around all stars selected (eps Eri, AD Leo, AU Mic) are dominated by the long-lived H^+ ion. In addition, planets in the Jeans escape regime also have a layer in which H_3^+ is the major ion at the base of the ionosphere. For fast-rotating planets, densities of short-lived H_3^+ undergo significant diurnal variations, their peak value being determined by the stellar X-ray flux. In contrast, densities of longer-lived H^+ show very little day/night variability and their value is determined by the level of stellar EUV flux. The H_3^+ peak in EGPs in the hydrodynamic escape regime under strong stellar illumination is pushed to altitudes below the homopause, where this ion is likely to be destroyed through reactions with heavy species (e.g., hydrocarbons, water). Infrared emissions from H_3^+ shall also be discussed, as well as the impact of stellar variability.

References

[1] Chadney, J., Galand, M., Unruh, Y., Koskinen, T., and Sanz-Foracada, J.: XUV-driven mass loss from extrasolar giant planets orbiting active stars. Icarus, 250, 2015.

[2] Sanz-Forcada, J., Micela, G., Ribas, I., Pollock, A., Eiroa, C., Velasco, A., Solano, E., and Garcia-Alvarez, D.: Estimation of the XUV radiation onto close planets and their evaporation. A&A, 532, 2011.

[3] Koskinen, T., Lavvas, P., Harris, M., Yelle, R.: Thermal escape from extrasolar giant planets. Phil. Trans. R. Soc. A., 372, 2014.

[4] Galand, M., Moore, L., Charnay, B., Mueller-Wodarg, I., and Mendillo, M.: Solar primary and secondary ionization at Saturn. JGR, 114, 2009.

EPSC Abstracts
Vol. 10, EPSC2015-340, 2015
European Planetary Science Congress 2015

The robustness of using near-UV observations to detect and study exoplanet magnetic fields

Jake D. Turner, Duncan Christie, Phil Arras, and Robert E. Johnson
Department of Astronomy University of Virginia, Charlottesville, VA 22904, United States (jt6an@virginia.edu)

Abstract

Studying the magnetic fields of exoplanets will allow for the investigation of their formation history, evolution, interior structure, rotation period, atmospheric dynamics, moons, and potential habitability. We previously observed the transits of 16 exoplanets as they crossed the face of their host-star in the near-UV in an attempt to detect their magnetic fields (Turner et al. 2013; Pearson et al. 2014; Turner et al. in press). It was postulated that the magnetic fields of all our targets could be constrained if their near-UV light curves start earlier than in their optical light curves (Vidotto et al. 2011). This effect can be explained by the presence of a bow shock in front of the planet formed by interactions between the stellar coronal material and the planet's magnetosphere. Furthermore, if the shocked material in the magnetosheath is optically thick, it will absorb starlight and cause an early ingress in the near-UV light curve. We do not observe an early ingress in any of our targets (See Figure 1 for an example light curve in our study), but determine upper limits on their magnetic field strengths. All our magnetic field upper limits are well below the predicted magnetic field strengths for hot Jupiters (Reiners & Christensen 2010; Sanchez-Lavega 2004). The upper limits we derived assume that there is an absorbing species in the near-UV. Therefore, our upper limits cannot be trusted if there is no species to cause the absorption.

In this study we simulate the atomic physics, chemistry, radiation transport, and dynamics of the plasma characteristics in the vicinity of a hot Jupiter using the widely used radiative transfer code CLOUDY (Ferland et al. 2013). Using CLOUDY we have investigated whether there is an absorption species in the near-UV that can exist to cause an observable early ingress. The number density of hydrogen in the bow shock was varied from $10^4 - -10^8\ cm^{-3}$ and the output spectrum was calculated (Figure 2) and compared to the input spectrum to mimic a transit like event (Figure 3). We find that there isn't a species in the near-UV that can cause an absorption under the conditions ($T = 1 \times 10^6$ K, semi-major axis of 0.02 AU, solar input spectrum, solar metallicity) of a transiting hot Jupiter (Figure 3). Therefore, our upper limits can not be trusted. We can eventually use CLOUDY to explore the escaping atmospheres from hot Jupiters. We can still use our data to constrain the atmospheric proprieties of the exoplanets.

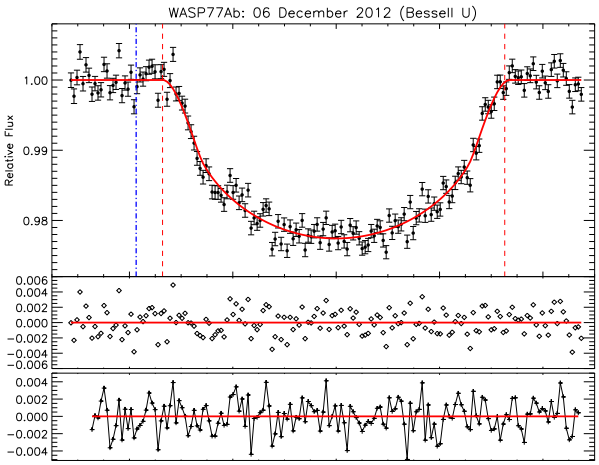

Figure 1: Near-UV light curve of WASP-77b (Turner et al. in press). The best-fitting model obtained from the EXOMOP is shown as a solid red line. The blue dot-dashed is a reasonable estimate of when the ingress should have started. The residuals are shown in the second panel. The third panel shows the residuals of the transit subtracted by the mirror image of itself. All our light curves show no near-UV asymmetries.

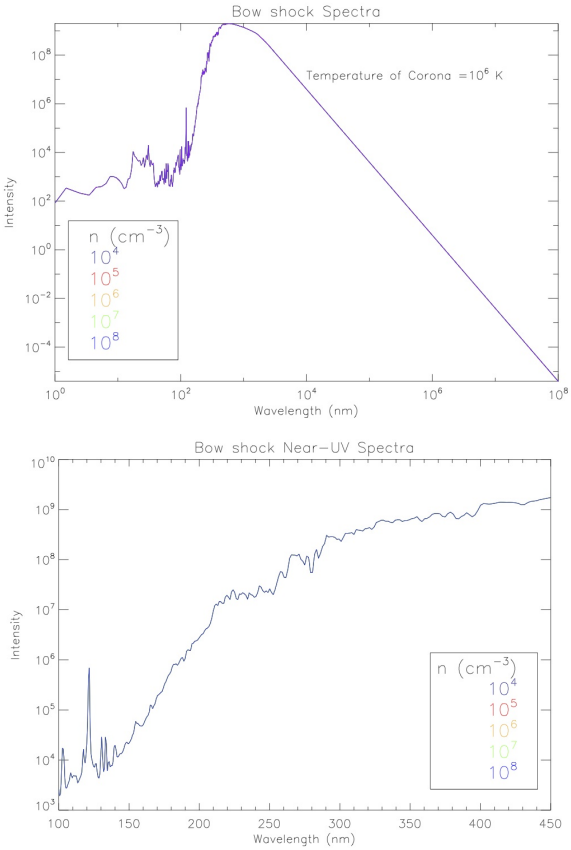

Figure 2: Output spectrum from CLOUDY of the bow shock at different number densities in the bow shock. **Top:** The full spectrum of the bow shock (x-ray to Radio). **Bottom:** The near-UV spectrum of the bow shock.

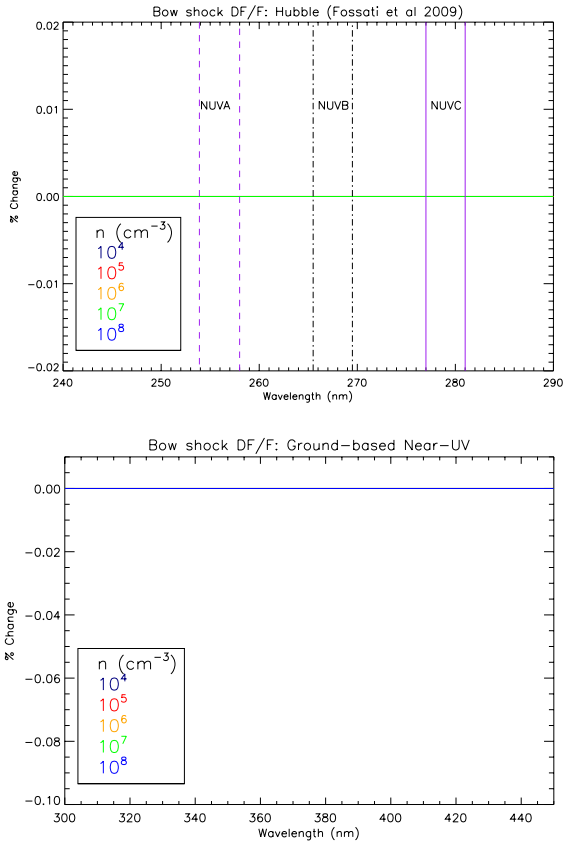

Figure 3: Change in flux of the output bow shock spectra at different number densities in the bow shock. We observe no detectable changes in flux due to a bow shock being in front of its host star. **Bottom:** Change in flux of the near-UV spectrum observed from the ground (300-440 nm; Turner et al. 2013; Pearson et al. 2014; Turner et al. in press). **Top:** Change in flux of the near-UV spectrum observed by Fossati et al. 2009 (the NUV filters are shown).

References

[1.] Ferland et al., RMXAA, 49, 137 (2013)

[2.] Fossati et al., ApJL, 714, L222 (2010)

[3.] Pearson et al., New Astro., 27, 102 (2014)

[4.] Reiners et al., AA, 522, A13 (2010)

[5.] Sanchez-Lavega, ApJL, 609, L87 (2004)

[6.] Turner et al., MNRAS, 428, 678 (2013)

[7.] Turner et al., MNRAS, In press (2015)

[8.] Vidotto et al., MNRAS, 411, L46 (2011)

Acknowledgements

We would like to thank the NASA Virginia Space Grant and Greg Ferland for all his help on using CLOUDY.

EPSC Abstracts
Vol. 10, EPSC2015-422, 2015
European Planetary Science Congress 2015

The habitability of terrestrial exoplanets with a time-marching climate model : an educational tool.

M. Turbet (1,2), F. Forget (1), J. Leconte (1) and C. Schott (3).
(1) Laboratoire de Météorologie Dynamique (LMD), Université Pierre et Marie Curie (UPMC), 4 place Jussieu, 75252 Paris, FRANCE (2) Ecole Normale Supérieure, Département de physique, 24 rue Lhomond, Paris, FRANCE (3) Labex ESEP (Exploration Spatiale des Environnements Planétaires), FRANCE **(mturbet@lmd.jussieu.fr).**

1. Introduction

Using a 1D version of the LMD Global Climate Model, we have developed a new educational tool (figure 1) which provides an accelerated simulation of the climate of terrestrial planets.

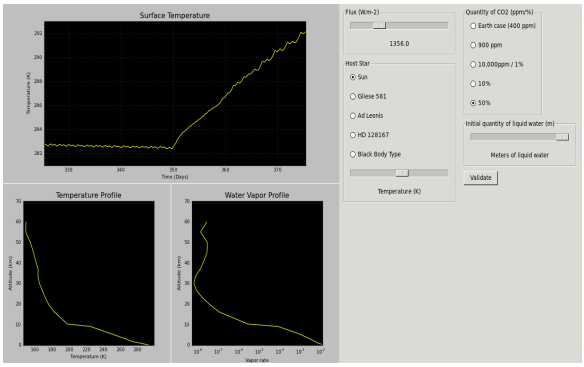

Figure 1 : Graphical User Interface of the 1D LMD GCM tool. It presents the evolution of the surface temperature and the instantaneous vertical profile of temperature and water vapor during a simulation which typically achieve 10 days per CPU seconds on a basic computer. Throughout the simulations, the star insolation (i.e. the distance from the star), the type of star, the amount of CO_2, ... can be modified.

This tool was designed for students to explore the "classical Habitable Zone", defined as the range of orbital distances within which a planet can maintain liquid water on its surface [1].

The inner edge of the Habitable Zone is the limit inside which runaway greenhouse occurs : For Earth-like planets with high stellar flux, surface liquid water tends to evaporate efficiently, releasing high amount of water vapor. This water vapor, which acts as a very strong greenhouse gas, leads to an increase of the surface temperature and thus to more evaporation.

The outer edge of the Habitable Zone is defined by a complete glaciation : For Earth-like planets with low stellar flux, at the limit where surface liquid water starts to freeze, ice forms and surface albedo increases. As a consequence, the amount of energy absorbed by the planet decreases, which reinforces the glaciation effect.

The 3D LMD GCM was previously used to reproduce these "runaway greenhouse" effect [2,3] and "runaway glaciation" effect [4,5,6].

To illustrate these concepts, we developed an educational – easy to use – 1D LMD GCM able to model these two limits and their dependencies with the type of star and the gas composition.

2. Description of the model

The GCM is designed for Earth-like atmospheres made of variable compositions of $N_2/O_2/CO_2/H_2O$ and includes a radiative transfer (correlated k method), a water cycle and a multiple-layers soil model. Wavelength dependency of ice albedo was taken into account according to Joshi et al (2012) [7].

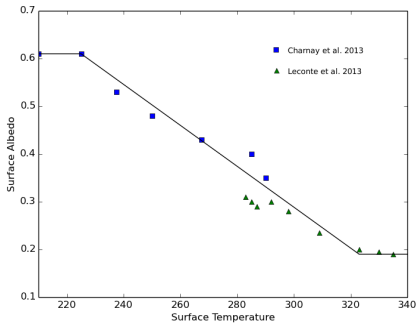

Figure 2 : Effective Surface albedo versus surface temperature. This empirical law was built according to a 3D parameterization of Earth atmosphere including the effects of clouds [2,6].

An empirical law between the global mean effective surface albedo and the global mean surface temperature (figure 2) was built from previous 3D LMD GCM simulations including the effects of clouds [2,6] and used as the surface albedo law for our 1D LMD GCM.

3. Use of the model

The user-friendly GCM tool we developed works with a Graphical User Interface shown on Figure 3. The code, mainly written in Fortran language, but wrapped in Python, is available on my webpage (http://www.lmd.jussieu.fr/~mturbet/). It only requires the GFortran compiler and the WX-python library.

Nonetheless, an online version of the tool will be soon available on http://www.esep.pro/.

4. Abilities of the model

The model faithfully reproduces the classical limits of the Habitable Zone, and their dependencies to the type of star/the gas composition. Furthermore, it provides an “hands on” experience by showing how the surface and atmospheric temperature as well as the profile of water vapor evolves through time when the external forcing (insolation, star spectrum) or the planet (quantity of CO_2, initial amount of water reservoir) is modified.

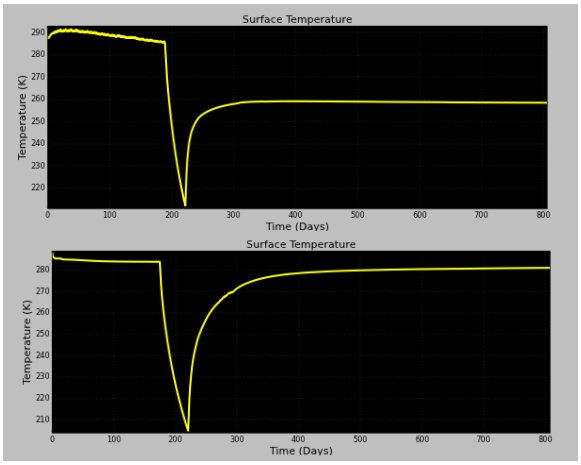

Figure 3 : Surface temperature versus time for a Sun-Earth system (top pannel) and a Mstar-Earth system (bottom pannel). At day 200, we cut the stellar flux. After 20 days, we put back the initial stellar flux.

Figure 3 shows for instance the ability of the model to deal with the runaway glaciation effect. Depending of the type of star, and thus the value of ice albedo, the Earth-like planet can/cannot be locked in a cold state.

The model is able to reproduce the runaway greenhouse effect beyond an insolation threshold of ~360 $W.m^{-2}$ in the case of the Sun-Earth system.

The GCM is also consistent with current Earth surface mean temperature.

Eventually, it would be easy to implement parameters like initial temperature pressure, excentricity/period of the orbit, mass/radius of the planet ... For these purposes, several versions of the tool will be available on my webpage.

The tool will be presented on demand during the poster session.

References

[1] Kasting et al. 1993, Habitable Zone around Main Sequence Stars. Icarus 101, 108-128.

[2] Leconte et al. 2013, Increased insolation threshold for runaway greenhouse processes on Earth like planets. Nature 504, 268-271.

[3] Leconte et al. 2013, 3D climate modeling of close-in land planets : Circulation patterns, climate moist bistability and habitability. Astronomy & Astrophysics, 554:A69.

[4] Wordsworth et al. 2011, Gliese 581D is the first discovered terrestrial-mass exoplanet in the Habitable Zone. The Astrophysical Journal Letters, 733:L48.

[5] Forget el al. 2013, 3D Modelling of the early martian climate under a denser CO_2 atmosphere : Temperatures and CO_2 ice clouds. Icarus 222, 81-99.

[6] Charnay et al. 2013, Exploring the faint young sun problem and the possible climates of the archean earth with a 3D GCM. Journal of Geophysical Research 118, 414-431.

[7] Joshi. M.M. & Haberle R.M.. Supression of the Water Ice and Snow Albedo Feedback on Planets Orbiting Red Dwarf Stars and the Subsequent Widening of the Habitable Zone. Astrobiology 12, 3-8.

EPSC Abstracts
Vol. 10, EPSC2015-430, 2015
European Planetary Science Congress 2015

Tidally-induced melting in extrasolar Earths

M. Běhounková (1), G. Tobie (2), G. Choblet (2), O. Čadek (1)
(1) Charles University in Prague, Faculty of Mathematics and Physics, Department of Geophysics, Czech Republic (2) Université de Nantes, Nantes Atlantique Universités, CNRS, Laboratoire de Planétologie et Géodynamique, UMR 6112, France (marie.behounkova@mff.cuni.cz / Fax: +420 221 912 555)

1 Introduction

The number of detected planets with mass and/or radius comparable to the Earth is now increasing. A large fraction of detected Earth-sized planets orbits at close distance from their stars ($P_{\rm orb} < 20\,{\rm days}$) [1]. Tidal interaction has likely played a major role in the evolution of these planets, especially during the early stage before the planets reached their final rotational state. Dissipation of tidal energy in the interiors during this early stage as well as in planets on eccentric orbits may strongly affect their thermal budget. Particularly for potentially habitable planets around low mass stars, it is crucial to understand how tidal friction may have affected their thermal and climate evolution, and whether it prevented the occurrence of stable and temperate surface conditions. In a previous study Behounkova et al. [2], we determined the conditions under which tidally-induced thermal runaways may occur for Earth-sized planets in 1:1 and 3:2 spin-orbit resonances around stars with mass varying between 0.1 and 1 solar mass. Here, we extend this analysis by taking into account the effect of melt production and transport. The objective is to quantify the extent and duration of large-scale melting events for planets entering thermal runaways regime, for a variety of initial conditions and orbital configurations.

2 Model

In order to investigate the effect of the tidal heating on the interior evolution and possible melt production, we perform numerical simulations in a three-dimensional spherical geometry using the numerical tool ANTIGONE [3, 2], solving simultaneously heat production by tidal friction and heat transfer by thermal convection. Compared to previous versions, the compression effect in the thermal equation was introduced and extended Boussinesq approximation is used. Due to large internal heating induced by tides, the temperature can reach the solidus [4, 5]. Therefore, internal melting and a simple model of instantaneous melt extraction has also been incorporated.

3. Results

Here, we present preliminary results for the model described above. For the example displayed in Figures 1 and 2, we investigate thermal evolution of strongly tidally heated exo-Earth assuming constant orbital parameters (1:1 spin-orbit resonance, $e = 0.005$, $P_{\rm orb} = 2\,{\rm days}$). The viscosity contrast and Rayleigh number has been chosen in order to mimic an efficiency of heat transfer comparable to the Earth. For simplicity, we consider a uniform surface temperature. Surface temperature variations due to stellar insolation and geothermal flux will be considered in a second step.

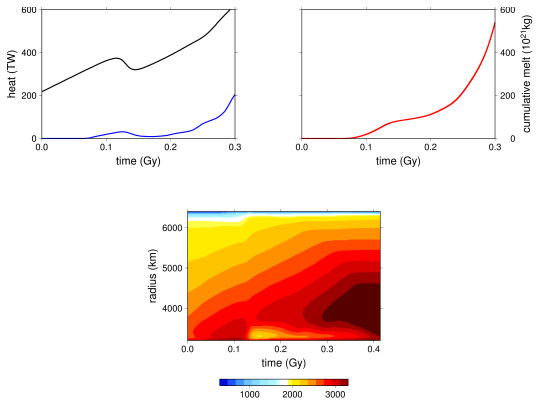

Figure 1: Example of the coupled tidal-thermal evolution of close-in Earth-like exoplanet; top left: evolution of tidal dissipation (black) and heat loss due to melting extraction (blue); top right: melt production; bottom: evolution of the average temperature; $Ra_{\rm bot} = 10^8$, $\Delta\eta = 150$, $h_{\rm rad} = 20\,{\rm TW}$, $Di = 0.5$, $\Delta T = 3000\,{\rm K}$, $T_{\rm S} = 300\,{\rm K}$, 1:1 spin-orbit resonance, $e = 0.005$, $P_{\rm orb} = 2\,{\rm days}$.

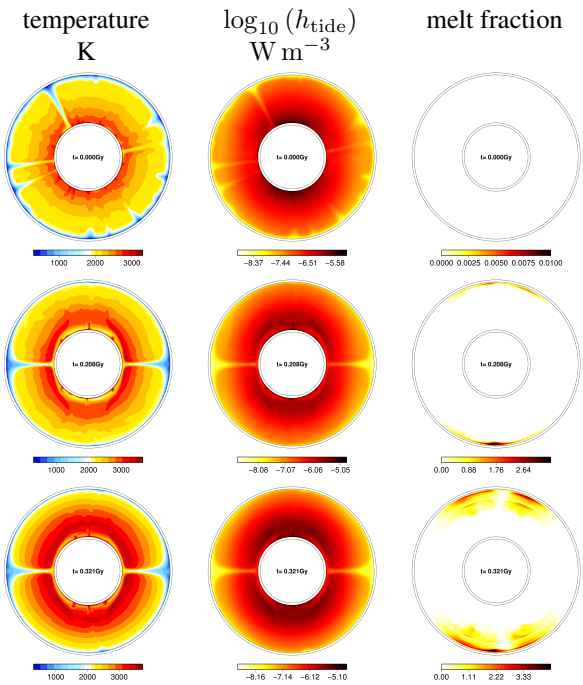

Figure 2: Snapshot of temperature field, tidal heating and fraction of melt, polar cross-section going through sub-stellar and anti-stellar points; model described in Figure 1.

The initial conditions for the simulation correspond to a statistical steady state of the system without any tidal heating. Once tidal heating is switched on ($t = 0\,\mathrm{Gy}$), a positive feedback between the temperature and the tidal heating is observed (see Figure 1). The dependence is not, however, monotonous as a mantle overturn occurs due to the low viscosity contrast and the increase of tidal heating with depth (Figure 2), leading to the formation of a low temperature zone above the core mantle boundary. Small scale upwellings are observed in this zone. Tidally induced melting first occurs at shallow depth in the polar regions ($t = 0.208\,\mathrm{Gyr}$, Figure 2). Then, the melt zone propagates downward and extend to lower latitudes ($t = 0.321\,\mathrm{Gyr}$). Interestingly, the warming and melting of the polar regions is accompanied by a migration of downwellings to the equator, as already observed in our previous study [2]. For this simulation with very strong tidal heating, even if melt extraction increase the surface heat flux (see Figure 1) and somehow limit the temperature increase in the polar region, no thermal equilibrium is reached at the end of simulation. The increase of global heating and average temperature even accelerate after $t = 0.25\,\mathrm{Gyr}$ (Figure 1).

Simulations with different initial states and orbital configurations will be presented during the conference, and the implications for the thermal evolution of close-in Earth-like planets will be discussed.

Acknowledgements

This work was supported by the CSF project No. 14-04145S.

References

[1] Batalha *PNAS* 111 (35), 12647–12654 (2014)

[2] Behounkova et al. *ApJ* 728, 89–+ (2011)

[3] Behounkova et al. *J. Geophys. Res.* 115 (E14), 9011–+ (2010)

[4] Litasov and Ohtani *Phys. Earth Planet. Inter* 134, 105–127 (2002)

[5] Andrault et al. *Earth and Planetary Science Letters* 304, 251-259 (2011)

EPSC Abstracts
Vol. 10, EPSC2015-475, 2015
European Planetary Science Congress 2015

Effect of flares on the chemical composition of exoplanets atmospheres

O. Venot (1), and L. Decin (1)
(1) Instituut voor Sterrenkunde, Katholieke Universiteit Leuven, Celestijnenlaan 200D, 3001 Leuven, Belgium (olivia.venot@ster.kuleuven.be), (2)

Abstract

M stars are very abundant in our Galaxy, and very likely harbour the majority of planetary systems. But a particularity of M stars is that they are the most active class of stars. Indeed, they experience stellar variability such as flares. These violent and unpredictable outbursts originate from the photosphere and are caused by magnetic processus. During such an event, the energy emitted by the star can vary by several orders of magnitude for the whole wavelength range. It results in an enhancement of the H_α emission and of the continuum. Different studies on the effect of flares on exoplanets have already been conducted [1, 2]. Here we are interested in the effect of a flare on the atmospheric composition of a warm Neptune orbiting around an M star. Using the stellar flux of AD Leo recorded during a flare event [1] and the chemical model of [3], we have studied the impact on the atmosphere. We have also computed the synthetic spectra assuming that such an event occurs during a transit. We will present these results.

Acknowledgements

O.V. acknowledges support from the KU Leuven IDO project IDO/10/2013 and from the FWO Postdoctoral Fellowship programme.

References

[1] Segura, A., Walkowicz, L. M., Meadows, V., Kasting, J., & Hawley, S.: The Effect of a Strong Stellar Flare on the Atmospheric Chemistry of an Earth-like Planet Orbiting an M Dwarf, Astrobiology, 10, 751, 2010

[2] Tofflemire, B. M., Wisniewski, J. P., Kowalski, A. F., et al.: The Implications of M Dwarf Flares on the Detection and Characterization of Exoplanets at Infrared Wavelengths, The Astronomical Journal, 143, 12, 2012

[3] Venot, O., Hébrard, E., Agúndez, M., et al.: A Chemical Model for the Atmosphere of Hot Jupiters, Astronomy & Astrophysics, 546, A43, 2012

EPSC Abstracts
Vol. 10, EPSC2015-671, 2015
European Planetary Science Congress 2015

THOR-ISO: a Global Circulation Model for Exoplanets on an Icosahedral Grid

J. Mendonça, S. Grimm and K. Heng
University of Bern, Center for Space and Habitability, Sidlerstrasse 5, CH-3012, Bern, Switzerland. Email: joao.mendonca@csh.unibe.ch

Abstract

In this presentation I will describe the details and first results of our new dynamical code for exoplanet atmospheres. This model is part of the Exoclimes Simulation Platform (ESP), and is a project of the Exoplanet and Exoclimes Group (see www.exoclime.org). The model I will present solves the complex physical and dynamical equations that include fundamental principles of atmospheric fluid dynamics and various idealisations of radiative transfer and dry convection, among others. I will also show the results of the first successful benchmark tests for this model, where we explore the results of the model for Earth-like and Hot-Jupiter like conditions. The analysis of the results from this complex and detailed model, will help us to have a better understanding of the diversity of climates and atmospheric circulations that we expect to find in the multitude of exoplanets already discovered.

1. Introduction

The study of extrasolar planets has become important since the discovery of a large number of these astronomical objects. The diversity of planetary characteristics observed raises questions about the variety of different climates. The influence of the astronomical and planetary bulk parameters driving new atmospheric circulations continues to be poorly understood. In the solar system the results from planetary spacecraft missions have demonstrated how different the planetary climate and atmospheric circulations can be. The study of exoplanets is going to require a study of a far greater range of physical and orbital parameters than the ones that characterise our neighbour planets of the solar system. For this reason the study of exoplanets will involve an even greater diversity of circulation and climate regimes.

The new model Thor-ISO is intended to be flexible enough to explore the large diversity of planetary atmospheres. The part of the model presented here includes the scheme which represents the resolved fluid dynamical phenomena in the atmosphere. In general the model solves the atmospheric fluid equations in a rotating sphere (fully compressible – nonhydrostatic system). The complex fluid equations are solved in a grid called icosahedral (see Fig. 1). A brief description of the methods used are included in the sections below. The results of the model are currently being analized and validated with other model results. These crucial experiments are explained in section 3.

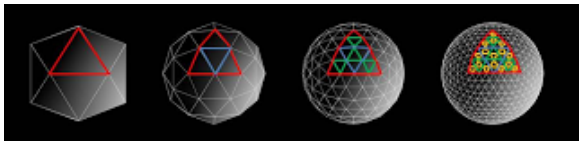

Figure 1: Model grid at different resolutions.

2. Model

The model developed solves the compressible Euler's equations:

$$\frac{\partial \rho}{\partial t} + \nabla \cdot (\rho \mathbf{v}) = 0, \quad (1)$$

$$\frac{\partial \rho \mathbf{v}}{\partial t} + \nabla \cdot (\rho \mathbf{v} \otimes \mathbf{v}) = -\nabla p - \rho g \hat{\mathbf{k}} - 2\rho\Omega \times \mathbf{v}, \quad (2)$$

$$\frac{\partial p}{\partial t} + \nabla \cdot (p\mathbf{v}) = -(\gamma - 1) p \nabla \cdot (\mathbf{v}) + (\gamma - 1) q_{heat} \quad (3)$$

where $\mathbf{v}$ is velocity, ρ is the density and p is the pressure. The equations solved by the model do not include any of the well knonw "traditional approximations", such as shalow atmosphere or hydrostatic approximation. The grid chosen to solve the equations is an icosahedral grid (Fig. 1), which is a quasi-uniform grid and avoids the so-called pole problem. To increase the numerical accuracy, smooth the grid distortions and move the points of the control volumes to the gravitational centres, we apply a "spring dynamic" method to the grid (Tomita et al 2001). The space

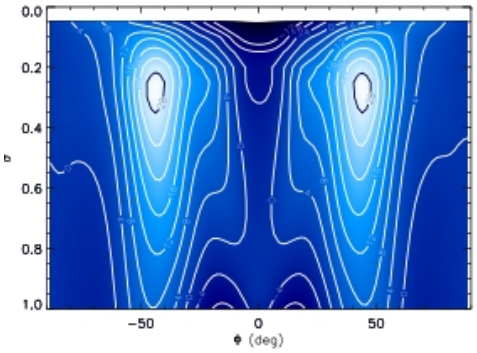

Figure 2: Earth benchmark test from Heng et al. 2000. The colours represent zonal winds averaged in time and longituude.

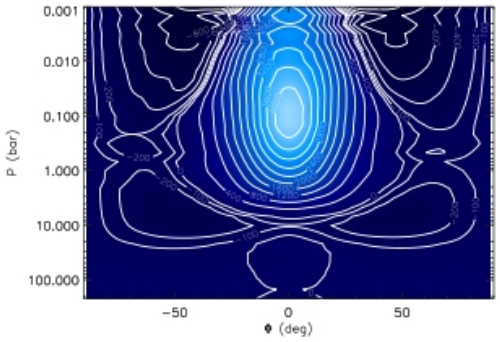

Figure 3: Hot-Jupiter benchmark test from Heng et al. 2000. The colours represent zonal winds averaged in time and longituude.

integration is based on a finite-volume method from Tomita and Satoh 2004. The time discretisation is based on a horizontally explicit and vertically implicit scheme. Using this method we avoid numerical instabilities due to the fast propagation of the sound waves in the tipically fine vertical resolution while keeping a reasonable time step.

To preserve numerical stability we include horizontal diffusion. This parameterisation removes the numerical noise and also represents the physical phenomena of eddy viscosity and turbulence on the subgrid scale. This model also allows us the possiblility to study deep atmospheres, which can be done by rescaling the equations by a factor which depends on the thickness of the atmosphere.

3. Three-dimentional test cases

This new model is aimed at probing a large range of planetary conditions. The two experiments explored represent a sample of this large diversity. We start exploring the "Held-Suarez" test which is an Earth benchmark test proposed in Held and Suarez 1994 and followed by a typically tidally locked hot-Jupiter benchmark test proposed by Heng et al. 2000. The results of the winds are expected to be similar to the ones shown in Fig. 2 and 3. Using our new model, we will show in this presentation how the results were achieved, what are the main mechanisms driving the atmospheric circulation in these planets and what are the advantages of using our new platform against the models that have been used recently to do exoplanet studies.

References

[1] Held, I., and Suarez, M.: A Proposal for the Intercomparison of the Dynamical Cores of Atmospheric General Circulation Models. Bulletin of the American Meteorological Society, vol. 75, Issue 10, pp.1825-1830.

[2] Heng, K., Menou, K. and Phillipps, P.: Atmospheric circulation of tidally locked exoplanets: a suite of benchmark tests for dynamical solvers. Monthly Notices of the Royal Astronomical Society, Volume 413, Issue 4, pp. 2380-2402 2000.

[3] Tomita, H., Satoh, M., Goto, K.: An Optimization of the Icosahedral Grid Modified by Spring Dynamics. Journal of Computational Physics, Volume 183, Issue 1, p. 307-331

[4] Tomita, H., and Satoh, M.: A new dynamical framework of nonhydrostatic global model using the icosahedral grid. Fluid Dynamics Research, Vol. 34, pp. 357-400, 2004.

EPSC Abstracts
Vol. 10, EPSC2015-677, 2015
European Planetary Science Congress 2015

Flows and magnetic fields in the convective interiors of tidally locked exoplanets

W. Dietrich (1), K. Hori (1), J. Wicht (2) and C.A. Jones (1)
(1) Department of Applied Mathematics, University of Leeds, Leeds, UK (2) Max Planck Institute for Solar System Research, Göttingen, Germany (w.dietrich@leeds.ac.uk)

Abstract

A large fraction of exoplanets orbit their host in synchronous rotation, hence the front side of the planet is strongly irradiated. We aim to understand the dynamic consequences for the convective flows and the dynamo process induced in the convective interiors subject to heterogeneous cooling. For exoplanetary gas giants the convective interior is part of the thick gaseous atmosphere, whereas for terrestrial planets we model the liquid part of the iron core. It is not understood, how such an outer boundary thermal anomaly is affecting the interior. Global, threedimensional dynamic models of convection and magnetic field induction might help to further develop a physical understanding of the interior properties and dynamics of exoplanets. As a first step, incompressible systems with and without competing radial convection should set a basis of more complex models taking various other characteristics, such as compressibility or inflation into account.

1. Introduction

We numerically investigate the convective interior as an incompressible, electrical conducting and rapidly rotating fluid contained in a spherical shell which is subject to internal heating and which outer boundary heat flux is varied along azimuth (see figure 1). The strong hemispherical temperature difference between front and back drives two strong azimuthal flow cells converging into a persistent and strong downwelling on the far side of the planet. Earlier analytical models suggested that the downwelling is phase shifted by 90 degrees eastwards to the terminator ([1], [2]). Our 3D fully nonlinear results confirm that prediction, but also characterise different regimes of the phase shift and the jet-like downwelling for sub- and supercritical convection. It is found, that for supercritical convection the position of the downwelling depends on various model parameters, such as the amplitude of the outer boundary heat flux anomaly. Further we discuss the interior flow and temperature structure and give an overview of the morphology of the induced dynamo fields.

2. Results

The combination of radial and horizontal temperature gradients will lead to a complex superposition of various flows. The heat flux anomaly is positioned such that, the hot mantle feature (and hence the host star) is on the right at $\phi = 0$, where then also the smallest amount of heat is extracted from the core as indicated by the small red arrows in the figure. Thus the largest CMB heat flux is at the opposite point (at $\phi = \pi$). Expectably, the boundary anomaly should drive a flow consisting of two cells, a (eastern) cold cyclone and a western hot anticyclone. The cells merge into an upwelling (downwelling) where the CMB heat flux is small (large).

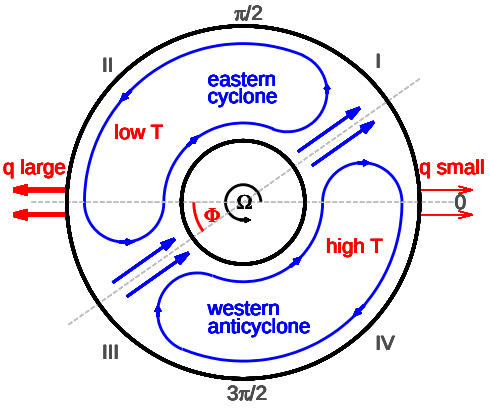

Figure 1: The horizontally varying outer boundary heat flux is mininal (maximal) at $\phi = 0$ ($\phi = \pi$).

A larger, but still subcritical Rayleigh number focusses the downwelling and smeares out the upwelling by temperature advection. Whereas a further enhanced Rayleigh number close to onset of convection allows

for buoyancy to take part, and the persistent downwelling migrates slightly backwards. We report methods to isolate and characterise the downwelling in time variable flows, overview the azimuthal distribution and 3D structure of mean flows, convection, temperature. Further we propose a scaling law for the amplitude of the downward jet. Finally, we investigate the structure of the emerging magnetic fields and how they alter the leading order force balance.

3. Summary and Conclusions

Our numerical results confirm the analytical predictions ([1], [2]), but show clearly that there are various further flow regimes depending on the unstable stratification [3]. For a realistic planet with a strong boundary anomaly the time-persistent jet-like downwelling might be phase shifted by ca. 30 degrees eastwards from the antistellar point seperating the hot western and cold eastern hemisphere. Hence the radial convection is much stronger at smaller azimuthal angles then the jet location, but almost suppressed eastward of it. This might have consequences for the magnetic field induction process as it relies on small scale, buoyant flows. When the heat flux variation is significantly smaller than the mean heat flux, the jet can move to much larger phase shifts. Further a scaling prediction suggest, that amplitude of the inward jet is at least on the order the global kinetic energy.

References

[1] Zhang, K., and Gubbins, D.M.: On convection in the earth's core driven by lateral temperature variations on the lower mantle, Geophys. J. Int., Vol. 108, 1992

[2] Yoshida, S. and Hamano, Y.: Fluid Motion of the Outer Core in Response to a Temperature Heterogeneity at the Core-Mantle Boundary and Its Dynamo Action, J. Geomag. Geoelctr., Vol. 45, 1993

[3] Dietrich, W., Wicht, J. and Hori, K.: Jet-like flows in the liquid cores of tidally locked terrestrial exoplanets, submitted to Astrophysical Journal, 2015

EPSC Abstracts
Vol. 10, EPSC2015-864-1, 2015
European Planetary Science Congress 2015

Stellar Winds and High-Energy Radiation: Evolution and influences on planetary atmospheres

C. P. Johnstone (1), L. Tu (1), M. Güdel (1), T. Lüftinger (1), H. Lammer (2), K. Kislyakova (2), B. Fichtinger (1), and the Pathways to Habitability project
(1) Department of Astrophysics, University of Vienna, Türkenschanzstrasse 17, A-1180, Vienna, Austria
(2) Space Research Institute, Austrian Academy of Sciences, Graz, Austria

Abstract

As part of the Austrian research network "Pathways to Habitability: From Disks to Active Stars, Planets and Life" (path.univie.ac.at), we study the evolution of stellar output (e.g. winds, high-energy radiation) over the lifetimes of solar-like stars and the influence of stellar output on the development of habitable planetary environments. We have developed a coupled stellar rotation-wind-radiation model that describes the long term evolution of stellar output over the course of a star's life. We show that the initial rotation rate of a star can significantly influence the evolution of winds and high-energy radiation and therefore the development of planetary atmospheres.

1. Introduction

The atmospheres of planets form and evolve embedded in the environments of their host stars. Stellar output includes winds, radiation, coronal mass ejections, high-energy particles, and magnetic fields. The most significant of these for the evolution of a planetary atmosphere are likely to be extreme ultraviolet (EUV) and X-ray radiation and stellar winds. EUV and X-ray radiation heat the upper atmospheres of planets and can cause significant expansion and, when the input stellar flux is high enough, hydrodynamic flow (Tian et al. 2005). The expansion of the upper atmosphere can lead to a large portion of the gas being exposed to the stellar wind, which can then lead to significant non-thermal erosion of the atmosphere (Kislyakova et al. 2014). These processes are highly sensitive to the properties of the stellar output.

Stellar rotation is the most fundamental parameter that drives magnetic activity (Wright et al. 2011), and therefore winds and radiation evolve on evolutionary timescales due to the evolution of stellar rotation. Stars start out their lives with a range of possible rotation rates spanning almost two orders of magnitude. As they age, they then rotate slower owing to their magnetised winds and this distribution of rotation rates converges: for solar mass stars, this convergence takes less than 1 Gyr.

2. Wind Evolution

A consequence of rotational evolution is the evolution of stellar winds. In Johnstone et al. (2015), we developed a rotation and wind model to predict the time evolution of the winds of stars with a range of masses. We estimated that the solar wind mass loss rate, $\dot{M}_\star$, depends on stellar rotation rate, $\Omega_\star$, radius, $R_\star$, and mass, $M_\star$, as $\dot{M}_\star \propto R_\star^2 \Omega_\star^{1.33} M_\star^{-3.36}$. For the solar wind, this leads to an approximate time dependence of the mass loss rate of $\dot{M}_\star \propto t^{-0.75}$ at ages older than 1 Gyr, and a range of possible evolutionary tracks at younger ages due to the spread in rotation rates (Fig. 1). With our model, we are also able to estimate the wind speeds and densities within a few AU of the star.

3. Radiation Evolution

In Tu et al. (2015), we combined our rotation model with a radiation model to predict the possible evolutionary tracks of solar-mass stars with different initial rotation rates. Stars starting out their lives at the 10th and 90th percentile of the rotational distribution remain highly active for <10 Myr and >200 Myr respectively. For several hundred million years, the differences in the X-ray and EUV luminosities between the two cases is more than an order of magnitude. This is shown in Fig. 2.

4. Summary and Conclusions

The different evolutionary tracks for solar mass stars can lead to differences in the evolution of planetary atmospheres. Tu et al. (2015) demonstrated this for the

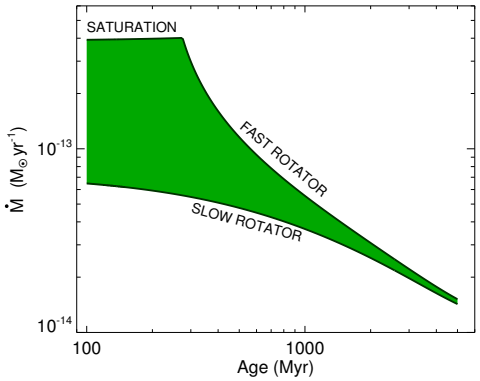

Figure 1: Figure reproduced from Johnstone et al. (2015) showing the predicted evolutionary changes of the solar wind mass loss rate. The slow and fast rotator tracks correspond to stars that are at the 10th and 90th percentiles of the rotational distributions.

simple case of a 0.5 $M_\oplus$ planet with a thick hydrogen envelope at 1 AU around a solar mass star. The atmosphere was assumed to be losing mass due to EUV and X-ray heating of the thermosphere. As we show in Fig. 2, if the planet orbits a rapidly rotating star, the example atmosphere loses its entire mass in 100 Myr. However, if the planet orbits a slowly rotating star, almost half of the initial atmospheric mass remains after 5 Gyr. Clearly, the star's initial rotation rate is an fundamentally important parameter for the development of terrestrial planetary atmospheres.

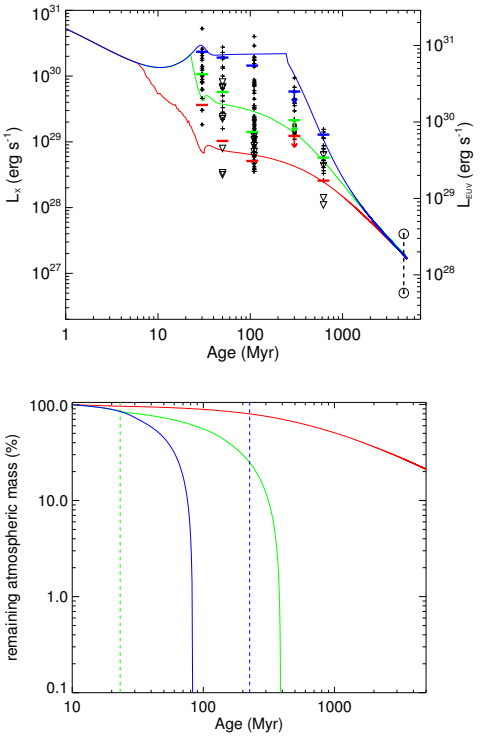

Figure 2: Figures reproduced from Tu et al. (2015). *Upper panel*: evolutionary tracks of the X-ray/EUV luminosities for stars at the 10th (*red*), 50th (*green*), and 90th (*blue*) percentiles of the rotational distribution. *Lower panel*: the corresponding evolutionary tracks for the atmospheric content of an example hydrogen dominated atmosphere of a 0.5 $M_\oplus$ planet.

Acknowledgements

The authors acknowledge the support of the FWF NFN project S11601-N16 "Pathways to Habitability: From Disks to Active Stars, Planets and Life", and the related FWF NFN subprojects S11604-N16 "Radiation & Wind Evolution from T Tauri Phase to ZAMS and Beyond" and S11607-N16 "Particle/Radiative Interactions with Upper Atmospheres of Planetary Bodies Under Extreme Stellar Conditions".

References

[1] Tian, F., Toon, O.B., Pavlov, A.A., De Sterck, H.: Transonic Hydrodynamic Escape of Hydrogen from Extrasolar Planetary Atmospheres, ApJ, Vol. 621, pp. 1049-1060, 2005

[2] Kislyakova, K.G., Johnstone, C.P., Odert, P., Erkaev, N.V., Lammer, H., Lüftinger, T., Holmström, M., Khodachenko, M.L., Güdel, M.: Stellar wind interaction and pick-up ion escape of the Kepler-11 "super-Earths", A&A, Vol. 562, A116, 2014

[3] Wright, N.J., Drake, J.J., Mamajek, E.E., Henry, G.W.: The Stellar-activity-Rotation Relationship and the Evolution of Stellar Dynamos, Vol. 743, id. 48, 2011

[4] Johnstone, C.P., Güdel, M., Brott, I., Lüfinger, T.: Stellar winds on the main-sequence II: The evolution of rotation and winds, A&A, Vol. 577, A28, 2015

[5] Tu, L., Johnstone, C.P., Güdel, M., Lammer, H.: The Extreme Ultraviolet and X-Ray Sun in Time: High-Energy Evolutionary Tracks of a Solar-Like Star, A&A (accepted), 2015

EPSC Abstracts
Vol. 10, EPSC2015-929, 2015
European Planetary Science Congress 2015

Chemical exchange in the interior of water-rich exoplanets

G. Tobie (1), G. Choblet (1), O. Grasset (1); (1): Laboratoire de Planétologie et Géodynamique, Université de Nantes, CNRS, France (gabriel.tobie@univ-nantes.fr)

Abstract

Since the discovery of the first exoplanet in 1995 [1], the number of detected exoplanets has grown nearly exponentially [2]. We have learnt from the existing dataset that our Solar System is rather unusual. Exoplanet surveys revealed notably that exoplanets intermediate between Earth and Neptune are surprisingly common, while notably absent in the Solar System [3]. Model mass-radius relationships indicate a great diversity of interior composition and atmospheric extent for the Super-Earth/Mini-Neptune-planet class [e.g. 4].

The observed continuum between Earth-sized and Neptune-sized planets challenges our understanding of planet formation and evolution, which has been biased for many years by our vision of the Solar System. Planetary worlds are probably much more diverse than originally thought, with a wide range of water and other volatile content. In the Solar System, there is a strong dichotomy between the inner system with dry planetary objects having a very small volatile fraction (<0.1 %), and the outer solar system where water ice constitutes a large fraction of solid phase (> 20%). The volatile contents among other systems likely vary more gradually, and a large fraction of exoplanets with sizes intermediate between Earth and Neptune may have a water content exceeding several percents.

The existence of massive water envelops around these planets may significantly affect the internal evolution and chemical exchanges between the deep interior and the atmosphere [e.g. 5]. Due to the very high-pressure expected inside these water-rich planets, especially for the the most massive ones, most of the water will be in the form of a high-pressure ice phase (ice VII) [6,7], the presence of liquid water being limited only to the first kilometres. The thermal structure and dynamics of these thick icy mantles are expected to control the heat and chemical transport from the silicate-rich interior to the surface [8,9], in a way analogous to the internal processes expected inside large icy moons like Titan and Ganymede [10]. At the temperature and pressure ranges expected in these thick icy mantles, most of volatile compounds are expected to be in a solid state, either trapped as clathrate hydrate, for example in the case of methane [11], or mixed with water ice, for example in the case of carbon dioxide [12]. The efficiency of chemical transport is therefore expected to be mostly controlled by the vigour of thermo-chemical convection.

By employing scaling laws derived from 3D numerical simulations of ice mantle dynamics [10] and phase diagrams constraining from high pressure experiments [11,12], we investigate the possible chemical evolution of planets by exploring a wide range of water content and planet size. We will discuss the impact of icy mantle dynamics on the thermal evolution of the deep interior as well as on the chemical exchanges between the deep silicate interior and the atmosphere.

Acknowledgements

This research received funding from the European Research Council under the European Community's Seventh Framework Programme FP7/2007-2013 grant agreement 259285.

References

[1] Mayor, M. & Queloz, D. (1995), Nature, 378, 355

[2] Batalha N. (2014) PNAS, 111, 1-8

[3] Marcy, G. W. et al. (2014) PNAS, 111, 12655.

[4] Howard, A. W. (2012), Science, 340, 572-576.

[5] Levi A. et al. (2013), Astrophys. J., 769:29.

[6] Léger, A. et al. (2004), Icarus, 169, 499.

[7] Sotin C. et al. (2007), Icarus, 191, 337-351.

[8] Fu, R. et al. (2010), Astrophys. J., 708, 1326.

[9] Levi, A. et al. (2014), Astrophys. J., 792, id. 125.

[10] Choblet, G. et al., *this conference*.

[11] Bezacier, L. et al. (2014), PEPI, 229, 144-152.

[12] Bollengier, O. et al. (2013), GCA, 119, 322-339.